Quantitative Aspects of Ventricular Repolarization:
Relationship Between Three-Dimensional T Wave Loop Morphology and Scalar QT Dispersion

Fabio Badilini, Ph.D., Jocelyne Fayn, Ph.D.,*
Pierre Maison-Blanche, M.D., Antoine Leenhardt, M.D.,
Marie Claire Forlini, M.S., Isabelle Denjoy, M.D.,
Philippe Coumel, M.D., and Paul Rubel, Ph.D.*

From the Department of Cardiology, Hôpital Lariboisière, Paris, and the *INSERM U121,
Hôpital Cardio-vasculaire, Lyon, France

Introduction: QT dispersion assesses repolarization inhomogeneity on 12-lead standard ECG. However, the implications of the electrical cardiac vector during the repolarization phase (the T wave loop) with the genesis of this phenomenon are unknown.

Methods and Results: The aim of this study was to explore conventional 12-lead resting ECG QT dispersion and the corresponding morphology of the spatial three-dimensional (3-D) T wave loop in 25 normals subjects, 30 postmyocardial infarction (MI) patients, and in 17 individuals with congenital long QT syndrome (LQTS). Standard and XYZ ECG leads were simultaneously digitized (250 Hz) and automatically analyzed. Ventricular repolarization dispersion was estimated by the range (RAN12o) and standard deviation (SD12o) of the 12 rate corrected QTo intervals (between the Q wave onset and the T wave offset). Spatial T wave loops were extracted from XYZ data and analyzed with a 3-D algorithm which provides quantitative parameters related to the loop morphology. All scalar measurements of dispersion were significantly larger in the two pathological populations; however none of them could discriminate post-MI from LQTS groups (RAN12o = 33.3, 61.4, and 62.7 ms respectively, for the three populations). Conversely, a loss of planarity and an increased roundness of the T wave loop were observed in the two pathological groups, with the former effect more pronounced in the LQTS (P = 0.04 compared to post-MI) and the latter in the post-MI group (P = 0.02 compared to LQTS). Furthermore, multiple regression and principal component analyses showed that planarity and roundness are independently involved with QT dispersion.

Conclusion: Changes in the morphology of the spatial T wave loop associated with QT dispersion were identified. These changes discriminate different substrates of repolarization inhomogeneity. The use of a 3-D technique to assess repolarization inhomogeneity may bring additional information on the intrinsic nature of this disorder. **A.N.E. 1997;2(2):146-157**

QT dispersion; ventricular repolarization; electrocardiography; vectorcardiography; T wave loop

Historically, dispersion of repolarization is the phenomenon under which neighboring areas of the myocardium exhibit different timing in their action potential cycles.[1-6] Repolarization inhomogeneity has been observed within a wide variety of cardiac disorders and it has been shown to constitute a substrate for malignant ventricular arrhythmias.[5,7-15]

A quick and noninvasive evaluation of repolarization inhomogeneity is difficult to obtain. Indeed, repolarization dispersion should be best investi-

gated with invasive analysis by measurement of monophasic action potentials recorded in different sites of the heart.[1,3,6] Noninvasively, repolarization inhomogeneity was initially assessed by detailed body surface mapping involving more than 100 surface leads.[4,5,12] However, since several years, repolarization dispersion is indirectly assessed on the surface 12-lead ECG by means of the interlead QT variability (the so-called QT dispersion), which is defined as the difference in the QT interval durations measured on a maximum of 12 ECG leads.[11,16] Despite the reduced number of exploring sites, 12-lead QT dispersion is significantly correlated with dispersion of monophasic action potential durations[6] and it provides an important clinical tool in several myocardial pathologies.

Patients with cardiac diseases associated with ventricular arrhythmias have higher values of QT dispersion than normal subjects, particularly in postmyocardial infarction (MI)[8,16-18] and in long QT syndrome (LQTS) populations.[7,10,12] QT dispersion could also provide important information to evaluate the profile of antiarrhythmic agents. For instance, Hii et al.[9] showed that in patients with drug-induced (Class Ia) torsades de pointes (Tdp), QT dispersion was increased. In LQTS patients, Priori et al.[10] demonstrated that the magnitude of QT dispersion is related with the clinical status and could predict efficacy of beta-blocker. Reduction of QT dispersion was also found to be associated with successful thrombolytic therapy of acute MI.[8]

Despite the evidence of the clinical importance of QT dispersion, a standardization of its use has not yet been established,[19,20] the main cause being the difficulty in measuring the end of the QT interval (i.e., the end of the T wave) in conditions like biphasic, notched or U wave corrupted repolarization morphologies. Indeed, definitions vary from one study to another between the original Surawicz method (intersection of the tangent to descending T wave with isoelectric line) to more recent approaches involving more signal processing but without a well-demonstrated superiority.[21,22]

QT dispersion is an indirect estimation of repolarization inhomogeneity which, by its nature, is a spatial phenomenon. The scalar estimation of a spatial phenomenon may lack precision and it may be affected by geometrical, extracardiac influences. More critically, it is unlikely that 12-lead QT dispersion would discriminate between different substrates leading to dispersion, like a myocardial ne-

crotic scar in MI or a genetic mutation of membrane ion channels in LQTS. Intuitively, even if the measured QT dispersion can be of the same magnitude, its triggering mechanisms may have different implications in terms of prognostic value for ventricular arrhythmias. Thus, a new strategy to better discern these problems is needed.

This study was conducted to explore the link between the morphology of the spatial repolarization loop and conventional 12-lead QT dispersion in controls, after MI and in the congenital LQTS. The T wave loop morphology was assessed by classic geometrical parameters and analyzed both independently and in relation with two different definitions of scalar QT dispersion.

METHODS

Study Population

The study population consisted of 72 subjects belonging to 3 specific subgroups: 25 normals (age: 27 ± 7 years, 15 females); 30 post-MI patients (age: 55 ± 13 years, 6 females); and 17 subjects with LQTS (age: 27 ± 18 years, 9 females).

Control subjects were part of an ongoing protocol under which, after written inform consent, they were screened and identified as normal by physical examination, 12-lead ECG, and echocardiography. In addition, a negative exercise test was required for all subjects over 40 years. The post-MI group was recorded between day 30 and day 45 after the infarction. All patients underwent successful thrombolysis and were receiving beta-blocking therapy (atenolol). In terms of infarction site, the population was well distributed (anterior = 15, inferior = 11, lateral = 4). Mean left ventricular ejection fraction assessed by angiography was 53% (ranging 39%—69%). All LQTS patients were genetically linked to chromosome 11p15.5 and six were probands. At the time of recording, 12 patients were symptomatic and 5 were receiving beta-blocking therapy (nadolol). LQTS patients were part of an ongoing genetic study approved by the ethical committee of Pitié-Salpétrière Hospital (Paris, France), and each patient provided informed consent.[23]

Data Acquisition

All subjects were recorded with a MAC15 electrocardiograph (Marquette Electronics, Inc., Mil-

waukee, WI, USA), which acquires simultaneously 8 standard leads (6 precordial plus 2 limb leads) and 3 additional leads, which in our case were the Frank orthogonal derivations. The remaining four standard leads are internally calculated. For each lead, the recorder stores both a sequence of 10 seconds of ECG data and the median beat obtained during the sequence. All this data was digitized at 250 Hz with a resolution of 5 μvolt and transferred to a PC environment for scalar and three-dimensional (3-D) analysis.

Scalar Analysis

Quantitative scalar analysis was performed by a dedicated semiautomatic algorithm, which examines the QRS-T complex of each individual lead (median beat). Before performing quantitative ECG measurements, the input signal is filtered for noise artifacts and both the first derivative and the integral sequences of the QRS-T complexes are calculated. On the basis of these sequences, the algorithm automatically detects the position of onset and offset of the QRS complex and of the T waves by a methodology previously described.[24] The positions of these fiducial points can be displayed and eventually modified (or deleted) by the user in case of obvious misplacement. The algorithm provides a series of many quantitative ECG measurements. For this study, the time intervals between the QRS onset and T wave offset (QTo) and between QRS onset and T wave maximum (QTm) for each of the 15 available leads were selected. All these intervals were corrected according to the Bazett formula by using the mean RR interval of the 10-second ECG data acquired by the recorder. Finally, two different parameters of repolarization dispersion were then defined for both the QTm and QTo series of intervals: the range (max-min) of the 12 standard leads (RAN12o and RAN12m) and the standard deviation of the 12 standard leads (SD12o and SD12m). In general, the dispersion of a time interval can derive from the variability of both its beginning or its end points. However, in the context of QT dispersion, the interest resides entirely in the terminating point (either the apex or end of T wave) and variations due to QRS onset may be troublesome. For this reason, the QRS onset of all 15 leads was fixed beforehand, and only the apex and end of T waves were allowed to change. In this way, the analyzed parameters fully reflected the disper-

sion of a point within the repolarization phase and were not influenced by depolarization factors.

3-D Analysis

The 3-D analysis was performed by using an algorithm (applied to the digitized XYZ data), which has been previously described.[25] A main feature of this method is to evaluate a 3-D loop (in this study the T wave loop) in a space defined by its three principal axes of inertia.[25,26] In this space, the morphology of the loop is determined by the three eigenvalues relative to the principal axes: λ_1; λ_2; and λ_3. In general, the energy of the loop is concentrated in a plane defined by λ_1 and λ_2 (called the preferential plane) so that the value of the third dimension (λ_3) is small with respect to that of λ_1 and λ_2. Furthermore, in the preferential plane, the T loop is usually narrow (ellipsoidal shape), thus leading to a value of λ_2 smaller than the value.

In order to assess the shape of the T wave loop, the eigenvalues were first normalized as follows:

$$\lambda_{1n} = \frac{100\lambda_1}{\lambda_1+\lambda_2+\lambda_3} \quad \lambda_{2n} = \frac{100\lambda_2}{\lambda_1+\lambda_2+\lambda_3} \quad \lambda_{3n} = \frac{100\lambda_3}{\lambda_1+\lambda_2+\lambda_3}$$

Thus, λ_{1n}, λ_{2n} and λ_{3n} represent the percent of explained inertia in the three principal axes and $\lambda_{1n}+\lambda_{2n}+\lambda_{3n} = 100$.

The T loop shape in the preferential plane was quantified by a roundness parameter (RP) defined as RP = $(\lambda_{2n}/\lambda_{1n})^{1/2}$. This parameter provides an estimation of the loop narrowness in the preferential plane, the smaller RP the thinner the loop (theoretically, a perfectly round loop will have RP = 1).

The planarity of the loop was directly assessed by the value of λ_{3n}. In addition, two parameters of planarity were defined by considering the third coordinate (projection on the third axis) of each loop sample with respect to the preferential plane. These two parameters were ΔQ, which expresses the difference between the maximum and minimum values normalized by $\lambda_1+\lambda_2+\lambda_3$, and AVQ, which expresses the average value of the third coordinate also normalized by $\lambda_1+\lambda_2+\lambda_3$. For a globally planar loop (i.e., a loop fully contained in the preferential plane), $\lambda_{3n}=\Delta Q=AVQ=0$; the larger the loss of planarity, the larger λ_{3n}, ΔQ and AVQ. A schematic representation of 3-D parameters is given in Figure 1.
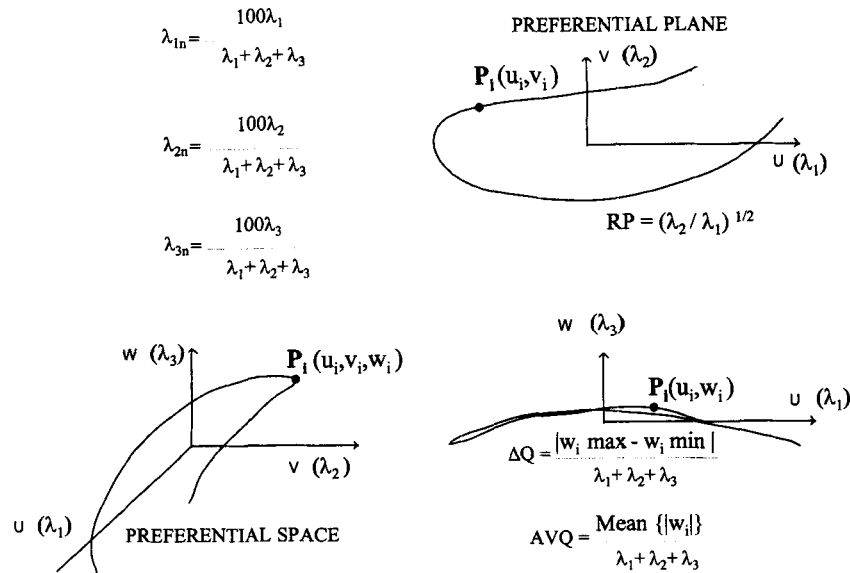
Figure 1. Schematic representation of 3-D parameters. In lower left panel, a T wave loop is drawn with respect to its axes of inertia u, v, and w. A digitized sample (P_i) on the loop is then characterized by three coordinate values relative to these axes: u_i; v_i; and w_i. The three eigenvalues λ_1, λ_2, and λ_3 (indicated in parentheses) provides information on the amount of inertia in each of the directions u,v, and w. The normalized eigenvalues λ_{1n}, λ_{2n}, and λ_{3n} express the percent of explained inertia for each of the directions. Upper right panel shows the projection of the loop on the preferential plane (plane formed by u and v axes) and provides a view of loop roundness whereas lower right panel is the projection on the plane formed by first and third principal axes (u and w) and gives an idea of loop planarity. See text for definition of all parameters.

Statistical Analysis

Intergroup Analysis

Differences of mean values of all scalar and 3-D dispersion parameters were compared between the two pathological populations and the normal population with Student's t-test.

Overall Analysis

To examine the link between scalar QT dispersion and 3-D morphology, the 72 subjects were first considered as a whole. Then, the correlations between global QT dispersion parameters (SD12o and RAN12o) and the 3-D morphological parameters were investigated with both univariate and multivariate stepwise regression analyses. Non-normalized eigenvalues (i.e., λ_1, λ_2, and λ_3 alone) were excluded, to avoid possible bias arising from miscalibrations among different recordings. For each of the scalar dispersion parameters, the best model with respect to the 3-D parameters was finally found.

Principal Components Analysis

To further explore the intercorrelations between the T wave loop morphology and scalar QT dispersion, a principal component analysis (PCA) was applied.[27] Variables assessed by the PCA were the global QT dispersion parameters (SD12o and RAN12o) and the three normalized eigenvalues together with the additional 3-D variables provided by the best regression model. The plots of the rotated factor loadings and of each individual factor scores in the plane of the first two principal components were visually assessed.

RESULTS

Intragroup Analysis: Pathological Groups Versus Normals

The ECG parameters of the three groups are given in Table 1. The mean RR intervals and all repolarization variables are significantly longer in the MI and LQTS populations when compared to normals. However, in the post-MI population this

Table 1. ECG Parameters

	Normals (n = 25)	Post-MI (n = 30)	LQTS (n = 17)	Post-MI vs LQTS
Age (years)	27 ± 7	55 ± 13**	27 ± 18	< 0.001
RR (ms)	910 ± 186	1063 ± 163**	1022 ± 128*	NS
QRS (ms)	87 ± 9	94 ± 8**	85 ± 7	< 0.001
QTo (ms)	377 ± 25	424 ± 34**	480 ± 46**	< 0.001
QTco (ms)	399 ± 21	413 ± 25*	475 ± 33**	< 0.001
QTm (ms)	301 ± 24	337 ± 29**	389 ± 33**	< 0.001
QTcm (ms)	319 ± 21	329 ± 23	386 ± 21**	< 0.001

Values are given as mean ± standard deviation; QTco and QTcm are the mean values of Bazett-corrected QTo and QTm intervals.
* $P < 0.05$ when compared to Normals.
** $P < 0.01$ when compared to Normals.

result is partially determined by a significantly increased QRS duration.

The results concerning scalar QT dispersion and T loop features are summarized in Table 2. All scalar dispersion parameters related to the T wave offset were significantly larger in the MI and LQTS patients when compared to the normal group. The correlation between SD12o and RAN12o was 0.96. Conversely, with the exception of SD12m in post-MI, the T wave apex dispersion variables did not discriminate among the three groups. Apex and offset dispersion variables were poorly correlated (SD12o vs SD12m, $r = 0.38$; RAN12o vs RAN12m, $r = 0.33$). Regarding the 3-D parameters, the MI and LQTS groups behave differently. In post-MI patients, only parameters related to the loop roundness (λ_{1n}, λ_{2n}, and RP), are significantly modified. Specifically, λ_{1n} is decreased (from 93% to 82%) and λ_{2n} is increased (from 6.7% to 17.2%). Both these changes lead to a parameter RP almost doubled

(from 0.24 to 0.44), thus indicating a rounder T wave loop associated with MI. On the contrary, the LQTS population shows significant differences in two of the parameters related to planarity (ΔQ from 0.5 to 0.75 and AVQ from 0.12 to 0.17). Of note, even in the most extreme case (an LQTS patient with apparent loss of planarity), the value of λ_{3n} was 1.23%. That is, the vast majority of the T wave loop is essentially contained in a plane.

Intergroup Analysis: Post-MI Versus LQTS

Comparisons between the MI and LQTS populations can be assessed by the significance levels in last columns of both Tables 1 and 2. Significant differences were found in both QRS and repolarization intervals (QRS is longer in post-MI; QTo, QTm, QTco, and QTcm are longer in LQTS). The two dispersion parameters were not different between the two populations (RAN12o = 61.4 vs 62.7 ms,

Table 2. Dispersion and T-loop Parameters

	Normals (n = 25)	Post-MI (n = 30)	LQTS (n = 17)	Post-MI vs LQTS
SD12o	9.98 ± 2.9	19.5 ± 6.5**	20.81 ± 14.9**	NS
RAN12o	33.3 ± 9.6	61.4 ± 20**	62.7 ± 37.5**	NS
SD12m	11.96 ± 5.2	16.4 ± 5.6**	15.68 ± 10.5	NS
RAN12m	44.6 ± 21.2	51.1 ± 16.7	49.7 ± 29	NS
λ_{1n}	93 ± 6.2	82 ± 12.1**	90 ± 12.3	0.04
λ_{2n}	6.7 ± 6.2	17.2 ± 12.0**	9.3 ± 12.2	0.04
λ_{3n}	0.19 ± 0.31	0.26 ± 0.25	0.37 ± 0.38	NS
ΔQ	0.5 ± 0.28	0.55 ± 0.32	0.75 ± 0.40*	NS
AVQ	0.12 ± 0.08	0.13 ± 0.07	0.17 ± 0.08*	0.04
RP	0.24 ± 0.13	0.44 ± 0.21**	0.28 ± 0.23	0.02

Values are given as mean ± standard deviation.
* $P < 0.05$ when compared to Normals.
** $P < 0.01$ when compared to Normals.

SD12o = 19.5 vs 20.81 ms, respectively, for post-MI and LQTS). On the contrary, all roundness variables were significantly different, λ_{2n} and RP being larger for the post-MI and λ_{1n} in the LQTS. Planarity variables (λ_{3n}, ΔQ and AVQ) were increased in LQTS patients. However, only AVQ reached statistical significance.

Overall Analysis

Table 3 depicts the correlation values obtained with linear regression analysis between the global QT dispersion variables and all the 3-D indices. In the last row, the correlations obtained with a stepwise multiregression analysis are given. Although all dispersion variables show higher correlations with roundness parameters, the best models always selected the combination of one parameter related to the planarity (ΔQ) and one parameter related to the roundness (λ_{1n}) of the T wave loop. The negative sign of the correlations with λ_{1n} means that a reduction of this parameter leads to an increased dispersion.

Figures 2, 3, and 4 give a representative example for a normal, a post-MI, and an LQTS subject, respectively. Both the T wave loop and the overlapped (and simultaneously recorded) 12 standard ECG leads are shown. The exaggerated roundness of the post-MI loop and the loss of planarity of the LQTS loop are noteworthy.

Principal Components Analysis

The 3-D variables used in the PCA were the normalized eigenvalues and ΔQ (since it was selected

Table 3. Correlations Between Dispersion Parameters and T Wave Loop Variables

	SD12o	RAN12o
λ_{1n}	-0.46 (< 0.001)	-0.41 (< 0.001)
λ_{2n}	0.45 (< 0.001)	0.41 (< 0.001)
λ_{3n}	0.36 (0.002)	0.37 (0.001)
ΔQ	0.29 (0.012)	0.31 (0.007)
AVQ	NS	0.27 (0.02)
RP	0.43 (< 0.001)	0.40 (0.001)
Best model	0.55 (< 0.001)	0.53 (< 0.001)
	$\lambda_{1n} + \Delta Q$	$\lambda_{1n} + \Delta Q$

P values are given in parenthesis.

by the multiregression analysis). The first two principal components explained 81% of the total variance. Figure 5 depicts the rotated factor loadings in the plane of these components. The first component mostly consists of λ_{1n} and λ_{2n} (thus reflecting the roundness effect), whereas the second component is clearly associated with λ_{3n} and ΔQ (thus reflecting the planarity effect). The dispersion variables SD12o and RAN12o are very close, as they are highly correlated ($r = 0.96$) and they lay at approximately 45° between the two principal components, thus indicating the complementary role played by T wave loop roundness and planarity in determining QT dispersion.

Figure 6 shows the projection of the different subjects in the principal component plane. All normal subjects are well clustered, whereas the post-MI patients are split in two groups: one which consists essentially of the inferior infarction site and which is rather overlapped with the normal cloud and another characterized by 12 of the 14 anterior MI. The cluster of LQTS is rather diffused.

DISCUSSION

This study is the first to explore the significance of spatial T wave loop changes associated with scalar QT dispersion. There are at least two specific T loop morphological features closely linked to QT dispersion: a rounder shape of the loop and a loss of planarity. The presence of two distinct spatial features linked to repolarization inhomogeneity is by itself a new finding. They may be related to different mechanisms of repolarization disturbances involved in the two pathological populations analyzed. Indeed, increased roundness is particularly clear in the post-MI group and the loss of planarity is more evident in the LQTS population.

Scalar Analysis Versus 3-D Analysis

Apart for the user visual validation of scalar fiducial points, which accounts for inaccurate measurement of uncommon T wave morphologies, the methodology used is fully automatic. Reproducibility of the results is close to 100% and all pitfalls that are known to affect manual measurement of QT dispersion on paper print-outs have been ruled out.[19, 20, 22, 28] Whatever the scalar dispersion parameter implemented as a response variable, the best

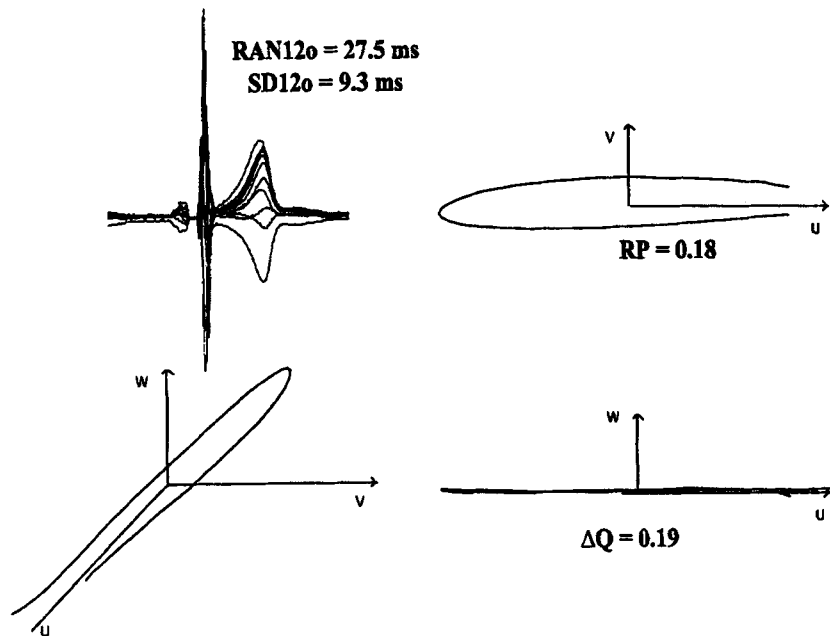RAN12o = 27.5 ms
SD12o = 9.3 ms

RP = 0.18

ΔQ = 0.19

Figure 2. Normal subject. Example of a T wave loop relative to a normal subject together with overlapped 12-lead ECG scalar leads (upper left panel). The 3-D loop is displayed in the lower left panel, whereas its projections on the preferential plane and on the vertical plane are respectively shown in the upper right and lower right panels. The typical slender and planar shape of the normal T wave loop (quantified by a small value of RP and ΔQ) can be appreciated.

model always selected a covariate related to the planarity of the T loop and a covariate related to its roundness (Table 3). Increased roundness is particularly striking in the post-MI whereas loss of

planarity seems largely involved with the LQTS population (Table 2). However, several post-MI also showed nonplanar loops and several LQTS had an enhanced roundness. The results of principal
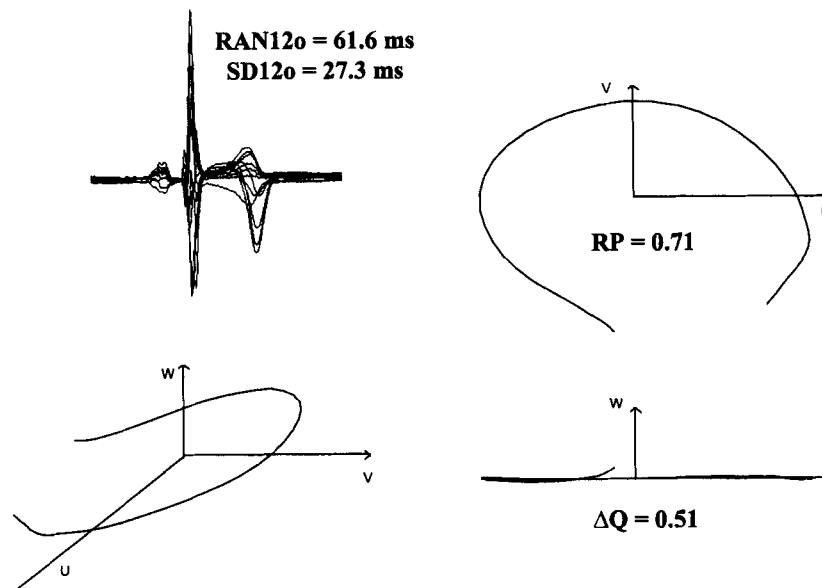
RAN12o = 61.6 ms
SD12o = 27.3 ms

RP = 0.71

ΔQ = 0.51

Figure 3. Post-MI patient. Example of a T wave loop relative to a post-MI patient together with overlapped 12-lead ECG scalar leads. The increased roundness of the loop (RP = 0.71) can be noticed. For more details, see legend of Figure 2.
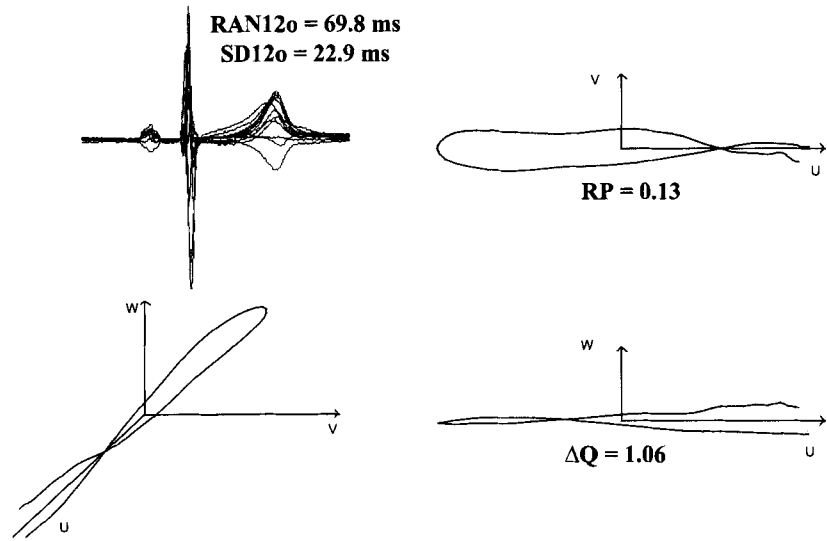
Figure 4. Long QT syndrome (LQTS) patient. Example of a T wave loop relative to an LQTS patient together with overlapped 12-lead ECG scalar leads. Despite a scalar QT dispersion comparable to that of post-MI patient of Figure 3, the T wave loop shape is completely different, with an exaggerated loss of planarity ($\Delta Q = 1.06$) and a roundness in the normal range. For more details, see legend of Figure 3.

component analysis strengthened these findings as they confirmed the complementary role played by the two morphological features (Fig. 5) as well as

their power in discriminating the three groups analyzed (Fig. 6).

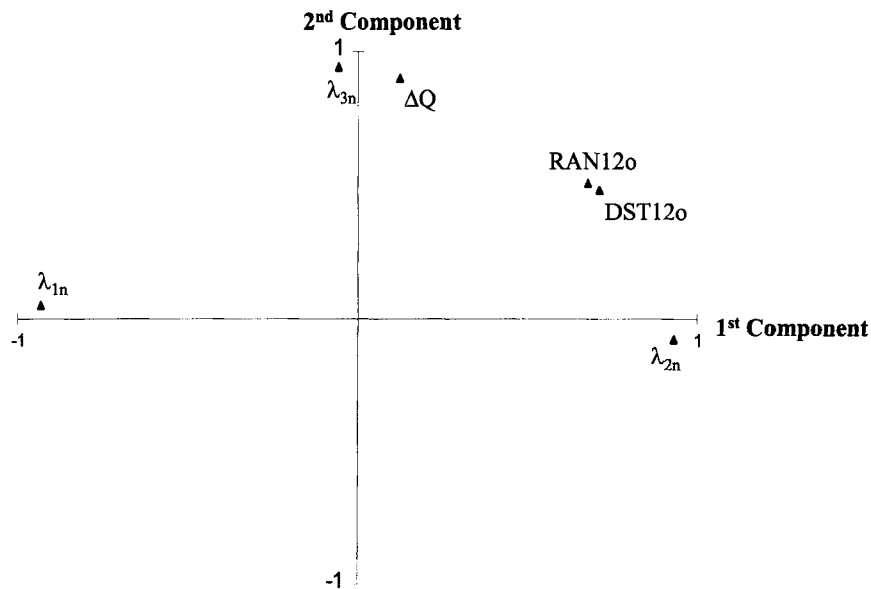Thus, the analysis of spatial T loop may provide

Figure 5. Principal component analysis: plot of rotated factor loadings in the plane formed by first two components. The coordinates of each variable (ranging from -1 to $+1$) give the correlation values of the variable with respect to the principal components. Note the high correlations of λ_{1n} and λ_{2n} with the first component and of λ_{3n} and ΔQ with the second component. See text for more details.
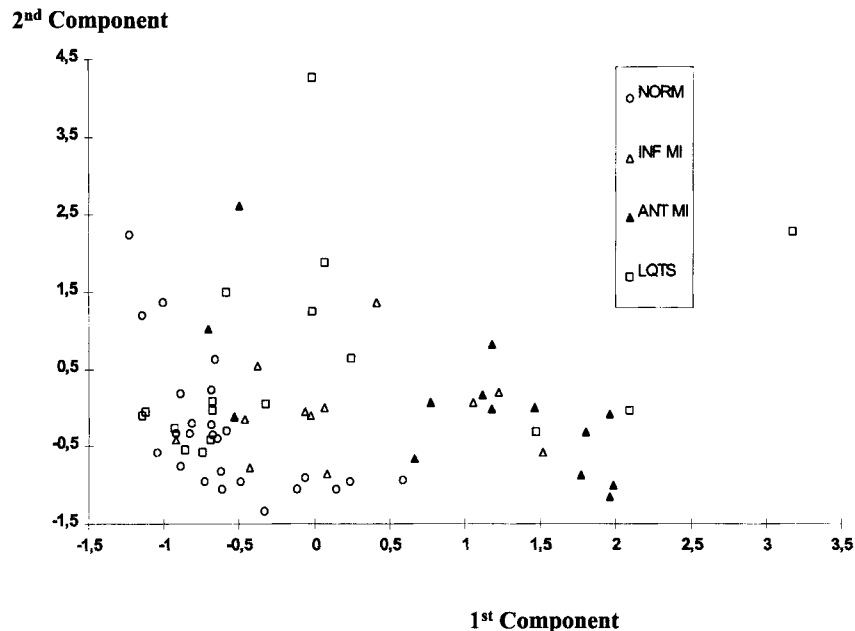
Figure 6. Principal component analysis: projection of all individuals in the plane formed by first two components. Post-MI are divided in two groups of inferior MI (INF MI) and anterior MI (ANT MI). The four lateral MI are not shown. See text for more details.

an alternative, noninvasive approach to assess repolarization inhomogeneity. Indeed, scalar techniques require the determination of each lead T wave offset, for which an accepted and reliable method has not yet been found. In this regard, the 3-D approach is certainly preferable as it avoids the scalar lead projection effects and, most importantly, it minimizes several technical flaws that are known to affect the evaluation of QT dispersion on the surface ECG.[19,22,28] However, as it has been shown in the field of diagnostic quantitative ECG for many pathologies,[29-32] the best performance may be obtained from the combined use of scalar and 3-D ECG (each method utilizing information neglected by the other one).

In this study, XYZ data had been processed according to their original purpose (i.e. the calculation of the vectorcardiographic spatial loop). On the contrary, recent applications implemented XYZ data in a pure scalar fashion, either deriving the so-called vector magnitude, for instance in late potentials detection, or merely using quantitative measurements performed on each single lead. The latter approach has been proposed as an alternative 3-lead QT dispersion, and its prognostic value had been demonstrated.[33] In this preliminary study, we

referred to dispersion as it was originally introduced (i.e., from the 12-lead ECG). However, we also calculated the corrected range of scalar XYZ lead QT intervals. As opposed to RAN12o, the range of XYZ could not discriminate controls and LQTS (mean values were 11.14 and 15.92 ms, respectively). In addition, correlations with the T loop were poor (no correlation at all with planarity).

Dispersion of QTm and QTo: Do They Provide the Same Information?

Due to the difficulty of QT interval automatic analysis, several systems have attempted to assess repolarization duration from measurements to the apex of the T wave.[34] From a purely technical point of view, we could not confirm the easier localization of T wave apex (both manually and automatically), particularly for the two pathological groups, which often showed biphasic and awkward T waves where proper location of apex was even more arduous than that of the offset. In addition, the respective weight of early and late repolarization phases is not yet fully established, at least for what concerns repolarization inhomogeneity.
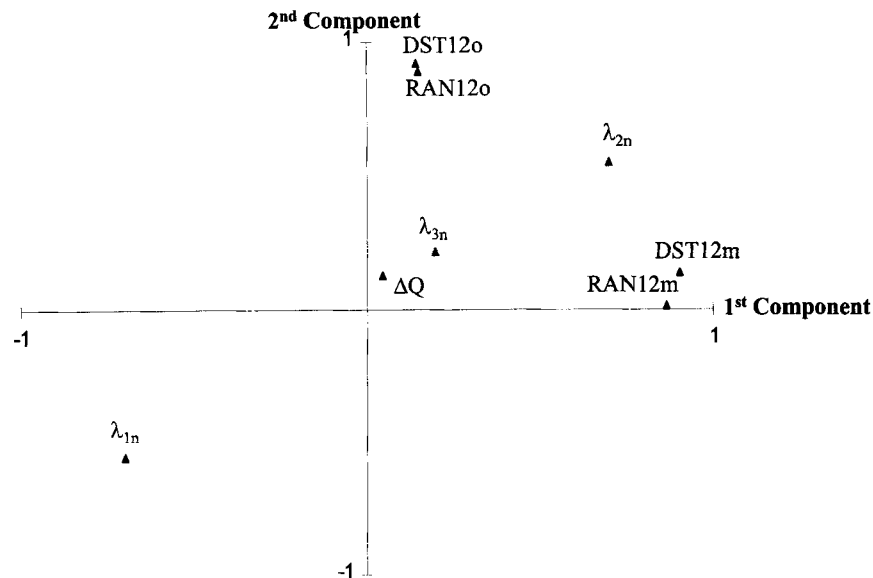
To answer these questions, we also investigated

Figure 7. Principal component analysis with apex dispersion variables added: plot of rotated factor loadings in the plane formed by first two components. See legend of Figure 5 and text for more details.

the link between the scalar apex dispersion and the 3-D variables. In general, correlation values were as good as those obtained with offset dispersion (the best model with SD12m selected λ_{3n} and RP as covariates, and the correlation value was 0.63). However, several results suggested a different significance associated with apex dispersion. First of all, the discrimination between controls and the two patient groups was weaker when using apex dispersion variables (SD12m could only separate post-MI and RAN12m none of the two groups). Second, all the correlations between apex and offset dispersion were poor (SD12o vs SD12m, r = 0.38; RAN12o vs RAN12m, r = 0.33). To further understand the significance of apex dispersion, we repeated the PCA analysis including SD12m and RAN12m. Due to the introduction of another cause of variability, the first two components only explained 72% of the total variance (as opposed to 81%). Figure 7 displays the rotated factor loadings in the plane of the first two components; apex and offset dispersion variables are respectively located very close to the two principal components while the morphotype parameters are in between. It is thus concluded that although they are both linked to the morphology of the T wave loop, offset and apex dispersion do not seem to reflect the same phenomenon, but rather they could be complementary one to each other.

Possible Mechanisms and Clinical Implications

In a 1983 study on dog monophasic action potential recordings, Kuo et al.[1] showed that large dispersion of repolarization creates an environment that facilitates the development of ventricular fibrillation when an early premature stimulus is applied. In the last 10 years many studies confirmed the link between QT dispersion and clinical outcome in many other pathologies.

In patients with MI, the differences between the longest and the shortest QT intervals are increased as compared to normal subjects and these modifications are related to the localization of the scar.[5] In addition, the interlead variation in QT interval is a useful predictor of ventricular arrhythmias[16,17] and is reduced after successful thrombolysis[8] or beta-blocking therapy.[13,16] Thus, increased QT dispersion following MI enhances susceptibility to arrhythmia and depends on both infarct site and reperfusion status. In this setting, the reentry substrate is related to the necrotic scar and to the surrounding borderline tissue.

In congenital LQTS, repolarization inhomogeneity is associated with higher risk of TdP,[7,12] and it can be reduced with effective beta-blocking therapy.[10] The role of early afterdepolarizations as a triggering phenomenon of torsades is clearly estab-

lished,[2,35,36] whereas the mechanism for the maintenance of torsades leading to ventricular fibrillation remains debated. A well-accepted hypothesis deals with the longer action potential durations of distinct layers of cells within the ventricular wall.[2] In LQTSs (either congenital or acquired), these longer action potential durations would be particularly exaggerated leading to an area of functional refractoriness that may act as a reentry circuit.[2]

According to these assumptions, the arrhythmia substrates that lead to repolarization inhomogeneity in the myocardium of post-MI and LQTS patients are not the same. However, in this study, the scalar dispersion of these two groups are in the same range of magnitude. Our results are the first to differentiate the two substrates, as shown by comparisons of λ_{1n}, λ_{2n}, RP, and AVQ in Table 2. We could hypothesize that in post-MI patients, QT dispersion is the reflection of a rounding of the T wave loop related to a myocardial scar. Conversely, in long QT patients, repolarization inhomogeneity is mostly the consequence of a decreased planarity of the T wave loop, related to the activity of mutated ion channels at individual myocardial locations.[2,37,38]

Limitations of the Study

The LQTS group was deliberately chosen among KVLQT1 genetically identified families for which the disease gene is a potassium cardiac channel and results obtained cannot be extrapolated to LQTS patients affected by other gene abnormalities. This is particularly true for LQT3-type patients, for which the morbid gene SNC5A encodes the cardiac sodium channel.[37,38] In addition, the range of age of LQTS was large, including three children below 10 years and an adult over 60 years. Regarding the post-MI group, all patients received thrombolysis and were treated with beta-blockers; consequently, the findings cannot be extrapolated to other post-MI populations. Furthermore, post-MI patients were older than the other two groups and had a male predominance.

The selection of two well-targeted groups does not reduce the main result of the study, (i.e., the existence of a correlation between scalar QT dispersion and morphological changes of 3-D T loop). Nevertheless, the finding of two different 3-D features characterizing post-MI and LQTS needs to be confirmed on larger populations. Another limita-

tion is the lack of follow-up of both post-MI and LQTS subjects and our inability to relate T wave loop changes to ventricular arrhythmias.

CONCLUSIONS

The findings of this study confirm the spatial nature of the T wave loop associated with scalar interlead variability. Twelve-lead QT dispersion is related to morphological distortions of the spatial 3-D T wave loop, which elicit an abnormal wavefront of repolarization. Both a loss of planarity and a rounder shape of the loop (more evident in the post-MI population) lead to conventional 12-lead QT dispersion. The respective weight of these two parameters can discriminate postinfarction and congenital LQTS substrates, which are undistinguishable with scalar analysis. These results suggest that in the field of quantitative ECG analysis, a 15-lead approach (12 standard leads + 3 orthogonal leads implemented in a 3-D dimension) should lead to a better understanding of repolarization inhomogeneity phenomena.

REFERENCES

1. Kuo CS, Munakata K, Reddy CP, et al. Characteristics and possible mechanism of ventricular arrhythmia dependent on the dispersion of action potential durations. Circulation 1983;67:1356-1367.
2. Antzelevitch C, Sicouri S, Litovsky SH, et al. Heterogeneity within the ventricular wall; electrophysiology and pharmacology of epicardial, endocardial and M cells. Circ Res 1991; 69:1427-1449.
3. Rosenbaum DS, Kaplan DT, Kanai A, et al. Repolarization inhomogeneities in ventricular myocardium change dynamically with abrupt cycle length shortening. Circulation 1991; 84:1333-1345.
4. Sylven JC, Horacek BM, Spencer A, et al. QT interval variability on the body surface. J Electrocardiol 1984;17(2):179-188.
5. Mirvis DM. Spatial variation of QT intervals in normal persons and patients with acute myocardial infarction. J Am Coll Cardiol 1985;5:625-631.
6. Zabel M, Portnoy S, Franz MR. Electrocardiographic indexes of dispersion of ventricular repolarization: An isolated heart validation study. J Am Coll Cardiol 1995;25:746-752.
7. Linker NJ, Colonna P, Kekwick CA, et al. Assessment of QT dispersion in symptomatic patients with the congenital long QT syndromes. Am J Cardiol 1992;69:634-638.
8. Moreno FL, Villanueva T, Karagounis LA, et al. Reduction in QT interval dispersion by successful thrombolytic therapy in acute myocardial infarction. Circulation 1994;90:94-100.
9. Hii JT, Wyse DG, Gillis AM, et al. Precordial QT interval dispersion as a marker of Torsade de Pointes. Circulation 1992;86:1376-1382.

10. Priori SG, Napolitano C, Diehl L, et al: Dispersion of the QT interval: A marker of therapeutic efficacy in the idiopathic long QT syndrome. Circulation 1994;89:1681-1689.
11. Day CP, McComb JM, Campbell RWF. QT dispersion: An indicator of arrhythmia risk in patients with long QT intervals. Br Heart J 1990;63:342-344.
12. De Ambroggi L, Negroni MS, Monza E, et al. Dispersion of ventricular repolarization in the long QT syndrome. Am J Cardiol 1991;68:614-620.
13. Cui G, Sen L, Sager P, et al: Effects of amiodarone, sematilide, and sotalol on QT dispersion. Am J Cardiol 1994;74: 896-900.
14. Barr CS, Naas A, Freeman M, et al: QT dispersion and sudden unexpected death in chronic heart failure. Lancet 1994;343:327-329.
15. Buja G, Miorelli M, Turrini P, et al: Comparison of QT dispersion in hypertrophic cardiomyopathy between patients with and without ventricular arrhythmias and sudden death. Am J Cardiol 1993;72:973-976.
16. Day CP, McComb JM, Matthews J, et al: Reduction in QT dispersion by sotalol following myocardial infarction. Eur Heart J 1991;12:423-427.
17. Higham PD, Furniss SS, Campbell RWF. QT dispersion and components of the QT interval in ischemia and infarction. Br Heart J 1995;73:32-36.
18. Yuan S, Wohlfart B, Olsson SB, et al: The dispersion of repolarization in patients with ventricular tachycardia. Eur Heart J 1995;16:68-76.
19. Statters DJ, Malik M, Ward DE, et al. QT dispersion: Problems of methodology and clinical significance. J Cardiovasc Electrophysiol 1994;5:672-685.
20. Kautzner J, Yi G, Camm J et al. Short- and long-term reproducibility of QT, QTc, and QT dispersion measurement in healthy subjects. PACE 1994;17:928-937.
21. Laguna P, Thakor NV, Caminal P, et al. New algorithm for QT interval analysis in 24-hour Holter ECG: Performance and applications. Med Biol Eng Comp 1990;28:67-73.
22. Glancy JM, Weston PJ, Bhullar HK, et al. Reproducibility and automatic measurement of QT dispersion. Eur Heart J 1996;17:1035-1039.
23. Dausse E, Denjoy I, Kahlem P, et al: Readjusting the localization of long QT syndrome gene on chromosome 11p15. Life Sci 1995;318:879-885.
24. Alberti M, Merri M, Benhorin J, et al. Electrocardiographic precordial interlead variability in normal individuals and patients with long QT syndrome. Comp Cardiol 1990:475-478.
25. Fayn J, Rubel P, Mohsen N. An improved method for the precise measurement of serial ECG changes in QRS duration and QT interval. Performance assessment on the CSE noise-testing database and on healthy 720 case-set population. J Electrocardiol 1991;24(Suppl):123-127.
26. Rubel P, Fayn J, Mohsen N. Stability of surface T wave and corrected QT interval in a normal male population. In GS Butrous, PJ Schwartz (eds): Clinical Aspects of Ventricular Repolarization. London, Farrand Press, 1989, p. 57.
27. BMDP Statistical Software Manual. BMDS Statistical Software, Inc., Los Angeles, 1992.
28. Murray A, McLaughlin NB, Bourke JP, et al. Errors in manual measurement of QT intervals. Br Heart J 1994;71:386-390.
29. Kors JA, van Herpen G, Willems JL, et al: Improvement of automated electrocardiographic diagnosis by combination of computer interpretations of the electrocardiogram and vectorcardiogram. Am J Cardiol 1992;70:96-99.
30. Willems JL, Abreu-Lima C, Arnaud P et al. The diagnostic performance of computer programs for the interpretation of electrocardiograms. N Engl J Med 1991;325:1767-1773.
31. van Bemmel JH, Kors JA, van Herpen G. Combination of diagnostic classifications from ECG and VCG computer interpretations. J Electrocardiol 1992;25(Suppl):126-130.
32. Chou TC. When is vectorcardiogram superior to the scalar electrocardiogram? J Am Coll Cardiol 1986;8:791-799.
33. Glancy JM, Garratt DM, Woods KL, et al. Three-lead measurement of QTc dispersion. J Cardiovasc Electrophysiol 1995;6:987-992.
34. Murray A, McLaughlin NB, Campbell RWF. Errors associated with assuming that the complete QT duration can be estimated from QT measured to the peak of the T wave. J Amb Monitoring 1995;8:265-270.
35. Levine JH, Spear JF, Guarnieri T, et al. Cesium chloride-induced long QT syndrome: Demonstration of afterdepolarization and triggered activity in vivo. Circulation 1985;72: 1092-1103.
36. Shimizu W, Ohe T, Kurita T, et al. Effects of verapamil and propranolol on early afterdepolarizations and ventricular arrhythmias induced by epinephrine in congenital long QT syndrome. J Am Coll Cardiol 1995;26:1299-1309.
37. Curran ME, Spiawski I, Timothy KW, et al. A molecular basis for cardiac arrhythmia: HERG mutations cause long QT syndrome. Cell 1995;80:795-803.
38. Wang Q, Shen J, Splawski I, et al. SCN5A mutations associated with an inherited cardiac arrhythmia, long QT syndrome. Cell 1995;80:805-811.